

Naval Research Laboratory

Washington, DC 20375-5000

2



NRL Memorandum Report 6575

X-Ray Spectra Produced by NaF Implosions

G. MEHLMAN,* D.A. NEWMAN* AND P.G. BURKHALTER

*Dynamics of Solids Branch
Condensed Matter and Radiation Sciences Division*

**Sachs/Freeman Associates, Inc.*

AD-A215 803

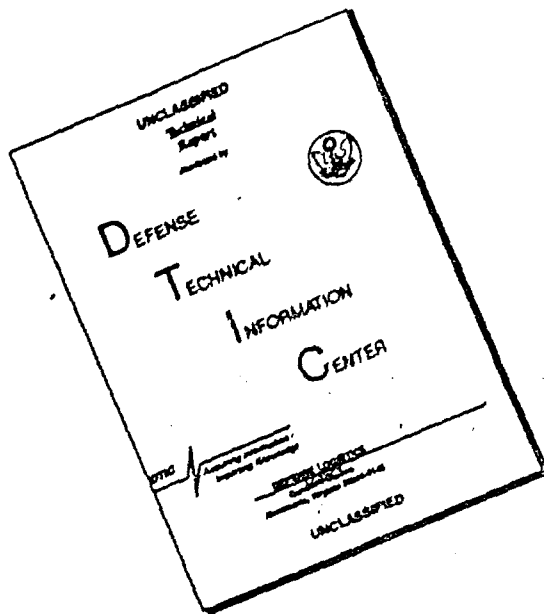
S DTIC ELECTE
DEC 28 1989 D
D CS D

November 13, 1989

Approved for public release; distribution unlimited.

89 12 27 049

DISCLAIMER NOTICE



**THIS DOCUMENT IS BEST
QUALITY AVAILABLE. THE COPY
FURNISHED TO DTIC CONTAINED
A SIGNIFICANT NUMBER OF
PAGES WHICH DO NOT
REPRODUCE LEGIBLY.**

SECURITY CLASSIFICATION OF THIS PAGE

Form Approved
OMB No 0704-0188

REPORT DOCUMENTATION PAGE															
1a REPORT SECURITY CLASSIFICATION UNCLASSIFIED		1b RESTRICTIVE MARKINGS													
2a SECURITY CLASSIFICATION AUTHORITY		3. DISTRIBUTION AVAILABILITY OF REPORT Approved for public release; distribution unlimited.													
2b DECLASSIFICATION/DOWNGRADING SCHEDULE		5 MONITORING ORGANIZATION REPORT NUMBER													
4 PERFORMING ORGANIZATION REPORT NUMBER(S) NRL Memorandum Report 6575		7a NAME OF MONITORING ORGANIZATION													
6a NAME OF PERFORMING ORGANIZATION Naval Research Laboratory	6b OFFICE SYMBOL (If applicable) Code 4680	7b ADDRESS (City, State, and ZIP Code) Washington, DC 20375-5000													
8a NAME OF FUNDING/SPONSORING ORGANIZATION Defense Nuclear Agency	8b OFFICE SYMBOL (If applicable)	9 PROCUREMENT INSTRUMENT IDENTIFICATION NUMBER													
8c ADDRESS (City, State, and ZIP Code) Washington, DC 20305-1000		10 SOURCE OF FUNDING NUMBERS <table border="1"> <tr> <td>PROGRAM ELEMENT NO 62715H</td> <td>PROJECT NO T99 QMXLA</td> <td>TAS NO</td> <td>WORK UNIT ACCESSION NO</td> </tr> </table>		PROGRAM ELEMENT NO 62715H	PROJECT NO T99 QMXLA	TAS NO	WORK UNIT ACCESSION NO								
PROGRAM ELEMENT NO 62715H	PROJECT NO T99 QMXLA	TAS NO	WORK UNIT ACCESSION NO												
11 TITLE (Include Security Classification) X-Ray Spectra Produced by NAF Implosions															
12 PERSONAL AUTHOR(S) Mehlman,* G., Newman,* D.A. and Burkhalter, P.G.															
13a TYPE OF REPORT Memorandum	13b TIME COVERED FROM _____ TO _____	14 DATE OF REPORT (Year Month Day) 1989 November 13	15 PAGE COUNT 20												
16 SUPPLEMENTARY NOTATION *Sachs/Freeman Associates, Inc.															
17 COSATI CODES <table border="1"> <tr> <th>FIELD</th> <th>GROUP</th> <th>SUB-GROUP</th> </tr> <tr> <td></td> <td></td> <td></td> </tr> <tr> <td></td> <td></td> <td></td> </tr> <tr> <td></td> <td></td> <td></td> </tr> </table>		FIELD	GROUP	SUB-GROUP										18 SUBJECT TERMS (Continue on reverse if necessary and identify by block number) Sodium implosions X-ray spectroscopy Plasma parameters	
FIELD	GROUP	SUB-GROUP													
19 ABSTRACT (Continue on reverse if necessary and identify by block number) <p>Spatially-resolved x-ray spectra were collected of imploding sodium plasmas using the Naval Research Laboratory Gamble 11 pulsed-power generator. A capillary-discharge was used as the source to inject sodium-fluoride plasmas for the fast Z-pinch implosion experiments.</p> <p>The plasma images recorded by curved-crystal spectrographs correspond to intense emission from a 3.5 cm long plasma column in the 4 cm interelectrode gap. Absolute emissivity values were obtained for the radiation emitted in the Na X and Na XI discrete transitions as well as for the total K-shell emission over the spectral range 800-1600 eV.</p> <p>Plasma parameters were determined from the measured spectral intensities compared to the ones predicted by plasma radiation theory. In regions near the nozzle, electron densities of several times 10^{21} cm^{-3} and electron temperatures of 200-300 eV are generated.</p>															
20 DISTRIBUTION AVAILABILITY OF ABSTRACT <input checked="" type="checkbox"/> UNCLASSIFIED/UNLIMITED <input type="checkbox"/> SAME AS RPT <input type="checkbox"/> DTIC USERS		21 ABSTRACT SECURITY CLASSIFICATION UNCLASSIFIED													
22a NAME OF RESPONSIBLE INDIVIDUAL P.G. Burkhalter		22b TELEPHONE (Include Area Code) (202) 767-2154 Code 4680													

CONTENTS

I. INTRODUCTION	1
II. ABSOLUTE LINE INTENSITY MEASUREMENTS	1
III. PLASMA THERMODYNAMICS	5
IV. RESULTS: SODIUM PLASMA PARAMETERS	9
A) Plasma Temperature Range	9
B) Ion Population Ratio	13
C) Plasma Density Range	14
V. CONCLUSIONS	14
VI. ACKNOWLEDGEMENTS	15
REFERENCES	16

Accepted For	
NTIS CRA&I	<input checked="" type="checkbox"/>
DOD TAB	<input type="checkbox"/>
Contractor	<input type="checkbox"/>
Distribution	
By	
Distribution	
Acknowledged	
Approved and for	
Dist	Special
A-1	

X-RAY SPECTRA PRODUCED BY NAF IMPLOSIONS

I. INTRODUCTION

Spatially-resolved x-ray spectra were collected for NaF plasmas produced by imploding sodium fluoride puffs with the Naval Research Laboratory Gamble II pulsed power generator (1). The motivation of this work has been the absolute measurement of the x-ray intensity in the heliumlike Na X 1s-2p line at 11.0027 Å (2) and the utilization of this x-ray line emission for resonant photopumping of the 1s-4p line in heliumlike Ne IX at 11.0003 Å (3). Such a scheme is the basis for a pulsed-power generated sodium-pump/neon-lasant soft x-ray laser.

This report presents the results of the x-ray spectral measurements. In Section II are the line and continuum intensity values for a sodium emitting plasma obtained in a selected NaF implosion with the Gamble II generator. In Section III the theoretical basis for plasma temperature derivation as well as a method for plasma density estimate are reviewed. In section IV the results for the sodium plasma parameters determined from the recombination continuum slopes, from selected line ratios, and from the measured lowering of the ionization threshold are presented.

II. ABSOLUTE LINE INTENSITY MEASUREMENTS

In the current work, the absolute emissivity values were obtained for the radiation emitted in the Na X and Na XI discrete transitions as well as for the total x-ray emission over the spectral range, 800-1600 eV. The interpretation of our spectra is based on the absolute line and continuum intensity measurements. These were compared with plasma radiation theory to

determine the temperature and density values for the regions of intense radiation in the interelectrode gap.

Atomic K-shell discrete transitions consist of the np--ls series of each heliumlike ion (F VIII and Na X) and each hydrogenlike ion (F IX and Na XI). The first lines of each ion main series are listed in Table I (wavelength λ in Å units) together with the line energy in eV and the transition probability, A, in 10^{12} s^{-1} . The line wavelengths for the hydrogenlike ions are taken from the computation of Garcia and Mack (4) while the lowest energy levels of the heliumlike ions are extracted from the tables of Ermolaev and Jones (5) which are based on refined calculations of two-electron ion states. The radiative probabilities, A, as well as energy values for the higher heliumlike levels, were computed using the atomic structure code provided by Cowan (6) although the hydrogenic values are obtained straightforwardly.

The experimental arrangement has been described previously (7) (8). The particular spectrum analyzed here was obtained with a distance of about 155 cm between the plasma and the KAP curved crystal and a space-resolving slit of 0.4 mm width. With this geometry the resolution in the plasma column is about 0.5 cm for the 4 cm interelectrode gap. The collected spectrum photograph is shown in Fig. 1 with the sodium major transitions indicated. The plasma image recorded by the spectrograph corresponds to a plasma column 3.5 cm long in the 4 cm interelectrode gap, in agreement with the pinhole image.

The measured absolute intensity values are given in Table II for several transitions of each ion. The line intensities were derived at three different locations in the interelectrode gap indicated in the first column. However, the tabulated values correspond to the total energy radiated by the whole 3.5

Table I
Fluorine and Sodium ion transitions

	1s ^{1/2} - 1s up			1s - np		
	F VIII			F IX		
	λ (Å)	E (eV)	A (10^{12} sec^{-1})	λ (Å)	E (eV)	A (10^{12} sec^{-1})
2	16,807	738	5.780	14,984	827	8.248
3	14,458	858	1.687	12,644	981	2.199
4	13,780	900	0.720	11,988	1034	0.870
5	13,487	919	0.378	11,707	1059	0.474
6	13,333	930	0.230	11,560	1072	0.279

	Na I X			Na I X1		
	λ (Å)	E (eV)	A (10^{12} sec^{-1})	λ (Å)	E (eV)	A (10^{12} sec^{-1})
1	11,703	11.27	13,827	10,026	1237	18,48
2	9,736	1315	3,467	8,459	1466	4,301
3	8,983	1380	1,679	8,021	1546	1,376
4	8,723	1411	0,874	7,832	1583	1,117
5	8,634	1426	0,525	7,735	1603	0,751

cm long plasma column regarded as uniform. The corresponding total energy radiated between 1100 and 1560 eV in this implosion is of the order of 250 joules. For this particular implosion there is disagreement between the spectral observations and the filtered XRD diagnostic. The latter is a factor of 3 higher.

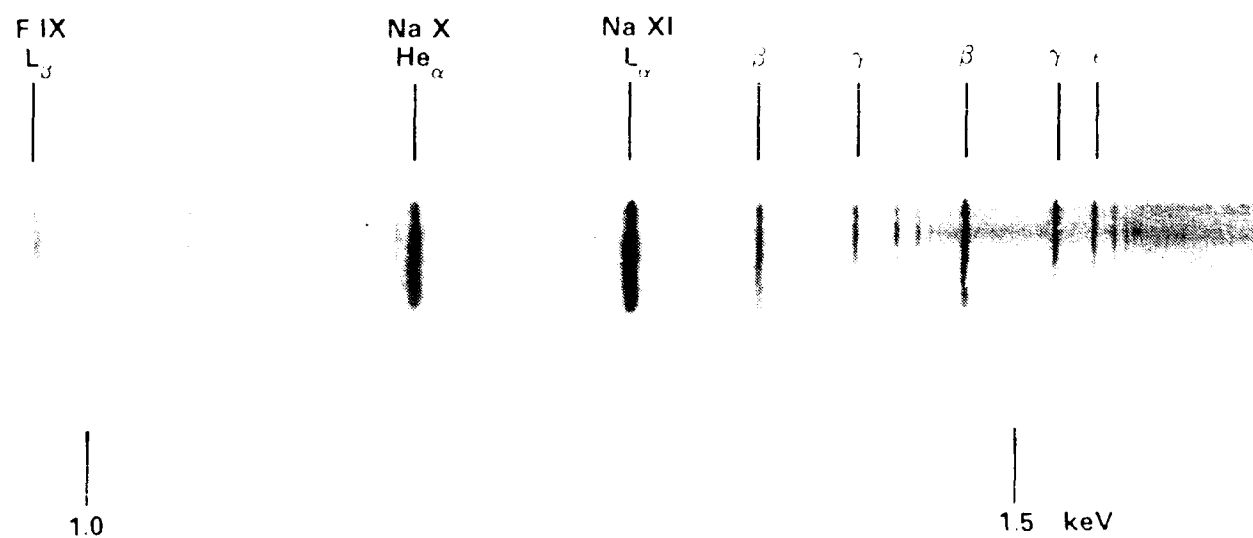


Figure 1. X-ray spectrum from a NaF implosion. The nozzle corresponds to the top of the spectral lines.

TABLE II
LINE INTENSITIES (JOULES into 4π sr)

Distance from nozzle (cm)	He- α	He- β	He- γ	L- α	L- β
0	26	10	6	34	9
1.6	56	16	8	84.5	12
3.2	32	8.5	3	46.5	7

III. PLASMA THERMODYNAMICS

A. Temperature Estimates

To estimate the plasma electron temperature, a standard spectroscopic method relies on measuring the recombination continuum "slope" using a log intensity plot versus photon energy.

The plasma electron temperature may also be derived from equating temperature-dependent theoretical line ratios to observed ones. The latter are derived from spectral traces, such as the one presented in Fig. 2, where the energy radiated in a given discrete transition is obtained by summing the intensity values over the line profile. Details for this derivation are given in Ref. 7. The trace shown in Fig. 2 is the average of eight scans performed along the entire spectral-line length.

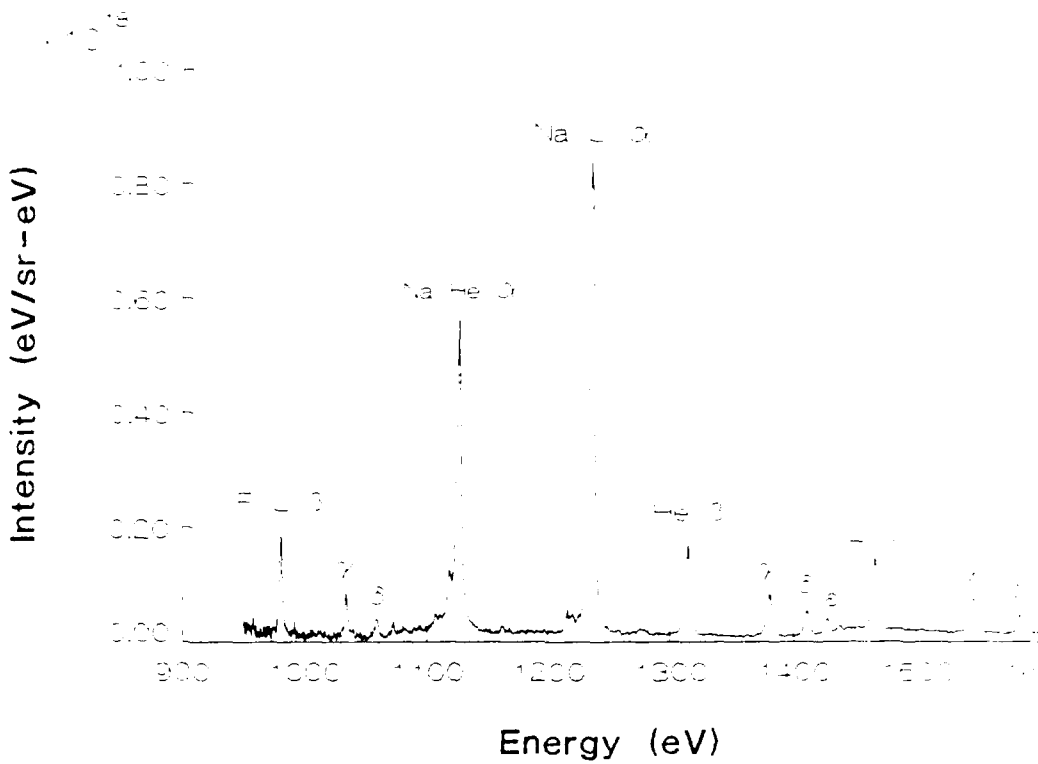


Figure 2. Absolute spectral intensity showing sodium heliumlike and hydrogenlike transitions (plus a few fluorine lines). On the vertical axis absolute intensities (on a linear scale) are to be multiplied by a geometry factor of 7.

To calculate line intensities, one confronts the problem of describing the distribution of the ions among the various stages of ionization in abundance and, among the various excited levels of each ion. Various plasma ionization models are commonly used (9) with accepted criteria of applicability. We shall restrict ourselves here, to a few line-intensity ratio predictions using different ionization equilibria according to the pair of excited levels involved in the ratio. In the three cases considered below the corresponding assumptions will be justified. In all cases, the predictions will be made assuming a large probability of escape through the plasma for the photons, i.e., in the so-called optically thin approximation.

(1) Thermodynamic equilibrium

Two discrete levels n, n' ($n < n'$) can be considered to be in thermal equilibrium if the electronic density, N_e , in the plasma reaches the value 10¹⁴:

$$N_e \geq 1.7 \cdot 10^{14} \sqrt{T_e} \cdot (\Delta E_{n,n'})^3$$

for N_e in cm⁻³, and plasma temperature, T_e , and energy level difference, $\Delta E_{n,n'}$, in eV. For all the levels of Na X and Na XI ions with $n > 1$, $\Delta E_{n,n'} \leq 80$ eV so for an "equilibrium" $T_e < 300$ eV, we can assume Boltzmann populations for the sodium np levels (except for $n=2$) provided:

$$N_e \geq 1.5 \cdot 10^{21}$$

(2) Collisionally-dominated equilibrium

It is reasonable to consider that the $n=2$ levels are mainly populated by electron-collisional excitation from the ground state. This so-called "coronal limit" equilibrium is valid for electron densities smaller than N_e^* with:

$$N_e^* = \frac{\sum_{j < n} A_{nj}}{\langle \sigma_{n-1} v \rangle}$$

with: j lower state, n excited state, A_{nj} radiative probability, $\langle \sigma_{n-1} v \rangle$ collisional deexcitation rate from level n to ground state in cm³/s. For these rates we used the parametric derivation of Sobelman, et al. (Ref. 1 p. 212) in the Coulomb-Born approximation. For the 2p level of the Na XI and F IX ions the N_e^* value is always higher than solid density for $T_e < 350$ eV.

With this model the line intensity (α and β transitions) is simply:

$$I_{n-1} = h\nu \times N_e n_i \langle \sigma_{n-1} v \rangle \cdot \frac{A_{n-1}}{\sum_j A_{nj}} \quad (1)$$

the last factor being -1 for the 2p levels. N_e is the electron density (cm⁻³).

and n_g is the number of ions in the ground state. The line intensity is expressed in the same units as the transition energy ($\hbar\nu$) per second.

This "coronal" approximation is reasonable to predict the α line intensities, for small optical depths in these transitions.

(3) Collisional-radiative equilibrium (2p and 3d levels)

A striking characteristic of the collisional excitation rates of hydroxide ions is the much larger magnitude of the 2p to 3d rate compared to the other rates (9) for plasma temperatures in the range 200-300 eV. This allows a simple description of the steady-state population distribution between the $n=1$ and $n=3$ levels of Na XI. This procedure is justified in a plasma with temperature around 300 eV and for electron densities in excess of $3 \times 10^{21} \text{ cm}^{-3}$ because below this value, collisional excitation of the 3p level from the ground state becomes predominant. With these conditions and neglecting ionization and recombination rates, we may include simply 2p-3d collisional excitation and de-excitation processes and radiative decays. The ratio of the intensities of L- α to L- β is thus written:

$$\frac{I_\alpha}{I_\beta} = R_{\text{LTE}}(1+\gamma)$$

where the factor γ represents departure from local-thermodynamic equilibrium (LTE).

$$\text{For Na XI : } R_{\text{LTE}} = 3.165 \cdot \frac{T}{228.7} \quad (\text{T in eV}) \text{ and:}$$

$$\gamma = \frac{0.136}{k} \cdot \sqrt{T} \cdot \frac{(228.7 + 0.418 T)}{228.7 + T}$$

We have used excitation rate parameters from Ref. 9; the electron density is expressed as $k \times 10^{21} \text{ cm}^{-3}$ and the plasma electron temperature, T, is in eV.

Table III gives predicted $\frac{L-\alpha}{L-\beta}$ intensity ratios for Na XI with this

model. These ratios were evaluated for temperatures of 200, 250, and 300 eV and for densities of 3×10^{21} and $5 \times 10^{21} \text{ cm}^{-3}$.

Table III Predicted line intensity ratios, $\frac{I(L-\alpha)}{I(L-\beta)}$, for Na XI

T_e eV	200	250	300
3	14.5	12	16.3
5	13	10	17

B. Density Estimates

The Coulomb interaction that binds the nucleus to the excited electron in an excited ion, may be screened by the surrounding ions and free electrons in a dense plasma. A major perturbation caused by this screening (Debye and Hückel 1923) is the lowering of the ionization limit and the cutoff of the number of bound states. In the sodium spectra, we observed a clear advance of the 1s np series limit for both Na X and Na XI ions with the highest lying level corresponding to $n=7$ or $n=8$. This is displayed in Fig. 3 where the measured ionization potentials for Na X perturbed by ionic or electronic pressure are indicated.

IV. RESULTS: Sodium plasma parameters

A) Plasma temperature range

1. Continuum slope measurements :

We have determined the plasma temperature from the recombination continuum

slopes at the end of the Na X series. The recombination continua are noticeable at the end of both the Na X and Na XI series (see Fig. 1). Fig. 3 shows three spectral traces in the region of the Na X recombination continuum corresponding to three different regions in the plasma. The intensity is plotted on a log scale so that the different slopes reflect the temperature variation. Linear fits to the continuum intensities are shown in this figure.

The continuum slope for the Na X continuum was measured because it is more intense. Depending on the position along the spectral image, we obtained temperatures varying from 210 to 290 eV. The highest corresponds to the region of most intense line radiation located about 1.6 cm from the nozzle for the particular implosion analyzed here. The lowest temperature corresponds to the region of most intense continuum emission originating from a clearly different location in the plasma column located 1.2 cm from the nozzle (see Fig. 3b). This continuum emission appears as a band across the spectrum (see Fig. 1) and seems to correspond to a very small spot-like volume of plasma. Also, another continuum emitting volume of minimum size appears adjacent to the nozzle.

Since the continuum radiation emission coefficient is proportional to the electron density square we estimate the density ratio between two regions of the plasma from the square root of the experimental ratio between the emission coefficients. Thus, we derive a density ratio of about 1.4 between the regions of peak continuum emission (Fig. 3b) and of maximum line radiation (Fig. 3c). This ratio is about the same as the reciprocal of the temperature ratio derived from the same plasma regions, indicating that the product $N_e \cdot T$ remains reasonably constant along the plasma, as described by Bennett's equation for magnetic pinches at equilibrium.

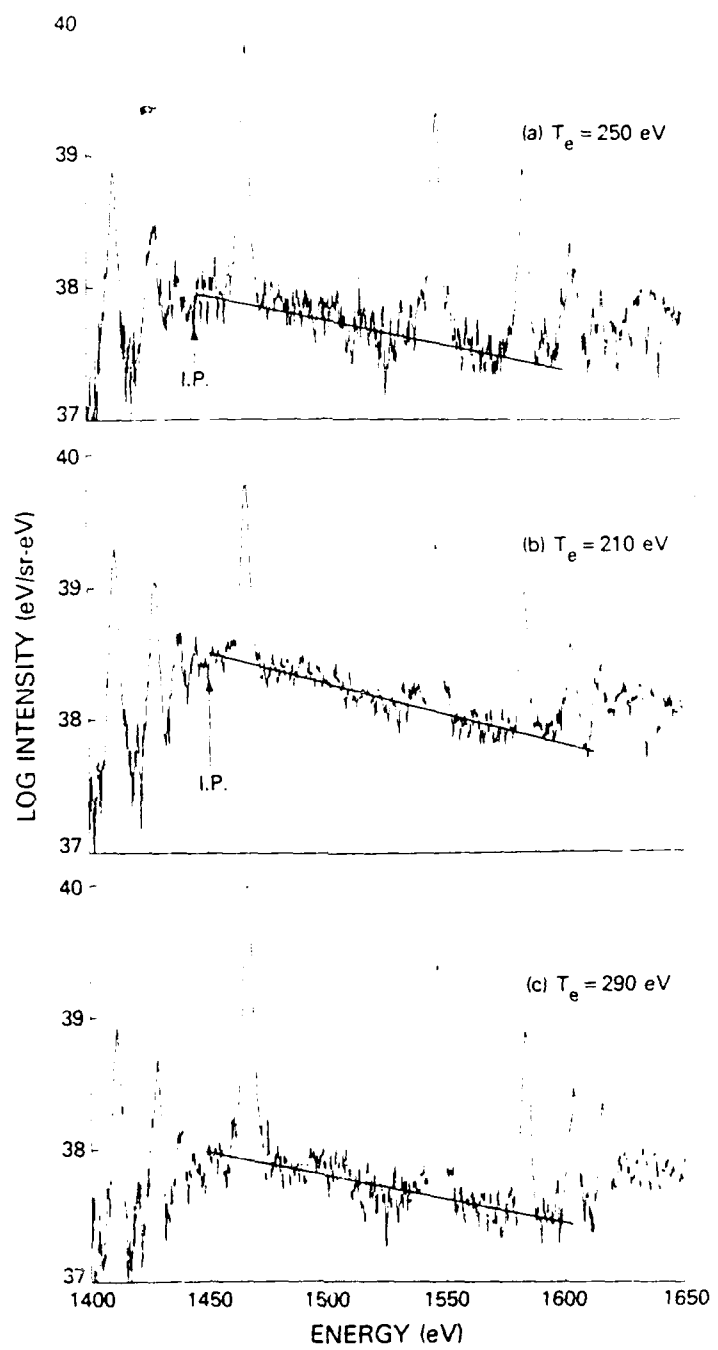


Fig. 3 Three processed scans from a spatially resolved spectrogram are shown. Each scan corresponds to a different plasma region: a) adjacent to nozzle, b) at 1.2 cm from nozzle, c) at 1.6 cm from nozzle. The natural log of the intensity versus photon energy is fitted linearly to the continuum between the x-ray lines. Plasma temperatures (T_e) are derived from the continuum slopes.

2.) Line intensity ratios :

In the region of most intense line radiation we note the relatively high intensity of the 1s - np series high n members for both ions . Values of line ratios for any two consecutive members appear lower than expected. For example, the $\frac{L-\alpha}{L-\beta}$ ratio varies from 7 to 9 in the electrode gap and decreases to as low as 4.5 near the nozzle compared to predicted values of 9 to 12 (see Table III). These values seem to indicate that, in the dense plasma regions, the line intensities are affected by time-dependent ion populations. In the region of intense continuum radiation the plasma density may be high enough (see below Sectio III C) to preclude coronal equilibrium or even 2p-3d CRE (see above section III A). The largest ratios for $\frac{L-\alpha}{L-\beta}$ of 7 to 9 correspond to temperatures in the range 220 - 290 eV with the LTE assumption, in general agreement with the preceeding observations.

The intensity of the higher members of the Na X $1s^2 - 1snp$ series, namely n=4 and n=5 was compared to L- α to derive very temperature - sensitive ratios for the L- α to He- γ or L- α to He- δ lines. Here, we assume that these np levels are in thermal equilibrium with the 1s level of Na XI and we use eq (1) to derive the L- α line intensity.

We obtain the following predicted line intensity ratios :

$$\frac{I(L-\alpha)}{I(He-\gamma)} = \frac{-1321}{T}$$

and

$$\frac{I(L-\alpha)}{I(He-\delta)} = \frac{-1290.5}{T}$$

$$\frac{I(L-\alpha)}{I(He-\delta)} = 4.28 \cdot T \cdot e$$

which allow an estimate of the temperature, T, by iteration. Measured $\frac{L-\alpha}{He-\gamma}$

ratios imply temperatures between 270 and 310 eV in the plasma near the nozzle. The minimum temperature is again ascribed to a region about 1 cm from the nozzle but appears higher than the lowest value obtained from the continuum slope, probably due to the limited spatial resolution in the plasma. As mentioned above, the continuum-emitting regions appear to be of very small dimensions compared to the regions responsible for intense line radiation.

Temperatures deduced from the $\frac{L-\alpha}{He-\delta}$ ratios are consistent with the preceding ones but are less accurate due to the weak intensity of the He- δ line.

B) Ratios of ion populations

1.) Ratio of L- α and He- α line intensity :

Using eq (1) to describe both α line intensities in the so-called "coronal" approximation we obtain :

$$\frac{I(L-\alpha)}{I(He-\alpha)} = \frac{n_{i+1}}{n_i} \cdot \frac{1.28}{0.59} \cdot \frac{e^{-109.56/T}}{e}$$

where n_{i+1} and n_i are the number of Na XI and Na X ions in their ground state, respectively, and the temperature, T, is in eV.

The population ratio $\frac{n_{i+1}}{n_i}$ computed from the experimental values of the α line ratio is close to 1 in the four plasma regions recorded on the nozzle side; the plasma temperature is taken from the continuum slope measurements. As a comparison point we note that in another NaF implosion with a comparable plasma temperature but a smaller α line intensity ratio,

the computed $\frac{n_{i+1}}{n_i}$ ratio was only around 0.5.

2.) Na XI np level populations:

From the 1s — np transition energy and radiative probability values for the Na XI ion (Table I), it is straightforward to obtain the relative populations of the np levels, in the optically thin case. All np levels with $n > 3$ appear almost equally populated with a slight minimum for the 3p one. The 2p level population is only about 2 to 2.5 times larger than that of the upper levels. It appears, again, that these population ratios could be accounted for with a model based on time-dependent plasma densities.

C) Plasma density range

From the traces obtained for the two regions of maximum continuum intensity we observed a largely depressed ionization potential from the electron pressure. Estimating conservatively from spectral traces such as the ones in Fig. 3, that the ionization limit is lowered to around 1450 eV while the theoretical one is at 1465 eV for Na X ions, we derived an estimate for the electron density using the formulation of Stewart and Pyatt (11).

A large value for the "local" density is found of the order of 3 to 4 10^{21} cm^{-3} . Again high electron densities seem to occur in spots of smaller dimension than the 5 mm spatial resolution.

V. CONCLUSIONS

Implosions of NaF plasmas with the Gamble II generator have produced from 40 to more than 400 joules in the Na X He- α transition. We have attempted to characterize the NaF plasma in terms of the temperature and density in the most intense radiative regions: the temperatures are in the range 210-300 eV

near the nozzle and there is evidence for minute spots of high electron density around 3 or 4 10^{21} cm $^{-3}$.

VI. ACKNOWLEDGMENTS

The authors wish to express appreciation to F.C. Young and S.J. Stephanakis of the Plasma Technology Branch for valuable discussions relating to the x-ray data.

REFERENCES

- (1) G. Mehlman, P.G. Burkhalter, D.A. Newman, V.E. Scherrer, S.J. Stephanakis, and F.C. Young, Bull. Am. Soc. 31, 1474 (1986).
- (2) P.G. Burkhalter, G. Mehlman, F.C. Young, S.J. Stephanakis, V.E. Scherrer, and D.A. Newman, J.de Physique 47, C6-247 (1986) and F.C. Young, S.J. Stephanakis, V.E. Scherrer, B.L. Welch, G. Mehlman, P.G. Burkhalter, and J.P. Apruzese, Appl. Phys. Lett. 50, 1053 (1987)
- (3) S.J. Stephanakis, et al., IEEE Transactions on Plasma Science, 16, 472 (1988).
- (4) J.D. Garcia and J.E. Mack, J. Opt. Soc. Am. 55, 654 (1965).
- (5) A.M. Ermolaev and M. Jones, J. Phys. B7, 199 (1974).
- (6) R.D. Cowan, J. Opt. Soc. Am. 58, 808 (1968); R.D. Cowan and D.C. Griffin, J. Opt. Soc. Am. 66, 1010 (1976).
- (7) G. Mehlman, P.G. Burkhalter, D.A. Newman, S.J. Stephanakis, F.C. Young, and D.J. Nagel, J. Appl. Phys. 60, 3427 (1986).
- (8) G. Mehlman, P.G. Burkhalter, D.A. Newman, S.J. Stephanakis, F.C. Young, and D.J. Nagel, NRL Memorandum Report No. 5833, July 1986
- (9) I.I. Sobelman, L.A. Vainshtein and E.A. Yukov, Excitation of Atoms and Broadening of Spectral Lines (Springer Verlag Berlin.. 1981).
- (10) R.W.P. McWhirter, Plasma Diagnostic Techniques (Acad. Press. New York, 1965) p. 206.
- (11) J.C. Stewart and K.D. Pyatt, Astrophys. Journ. 144, 1203 (1966).



DEPARTMENT OF THE NAVY
NAVAL RESEARCH LABORATORY
WASHINGTON, D.C. 20375-5600

ERRATA

4837-12-1

29 March 1990

From: Commanding Officer, Naval Research Laboratory

To: Distribution

Subj: ERRATA; NRL Memorandum Report 6575, entitled "X-Ray Spectra Produced by NaF Implosions," by G. Mehlman, D.A. Newman, and P.G. Burkhalter, dated November 13, 1989.

1. Page i, DD Form 1473, should be replaced with the corrected page i provided herewith.

- a. Section 8a - Defense Nuclear Agency is replaced with Strategic Defense Initiative Organization.
- b. Section 8c - ZIP Code 20305-1000 is replaced with 20365-1900.
- c. Section 10 - reference to Program Element No. and Project No. have been removed.

A handwritten signature in black ink that reads "Timothy D. Calderwood".

Timothy D. Calderwood
Head, Publications Branch